Appendix A. Supplementary Information

1. N_2 PHYSYSORPTION MEASUREMENTS OF CALCINED SAMPLES

FIG. A.1- Pore size distribution for calcined samples (NiO/Al_2O_3 (a), $NiO/MgAl_2O_4$-Al_2O_3 (b), $NiO/CaZrO_3$ (c) and $NiO/LaFeO_3$ (d)).

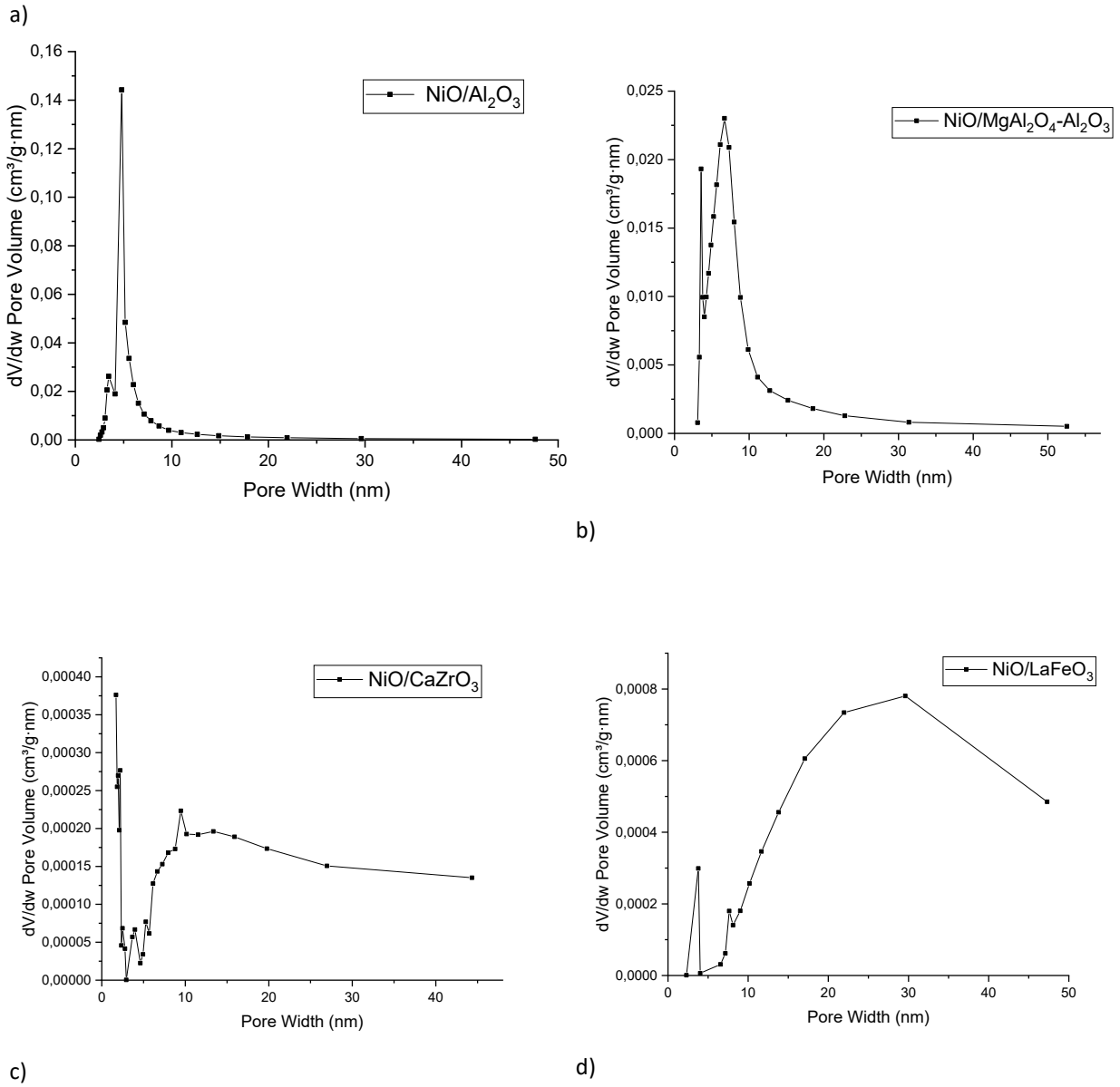

FIG. A.2- N_2-physisorption of NiO/Al_2O_3 (a), $NiO/MgAl_2O_4$-Al_2O_3 (b), $NiO/CaZrO_3$ (c) and $NiO/LaFeO_3$ (d) catalysts.

a)

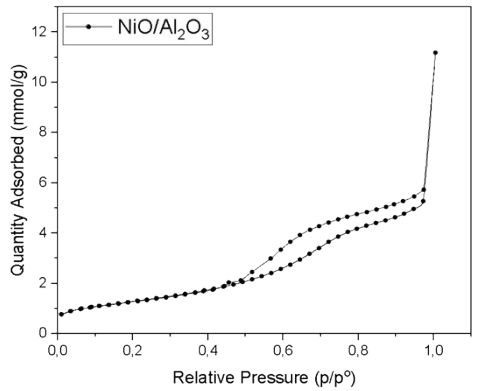

b)

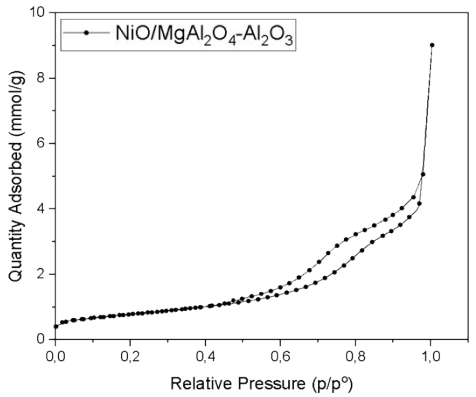

c)

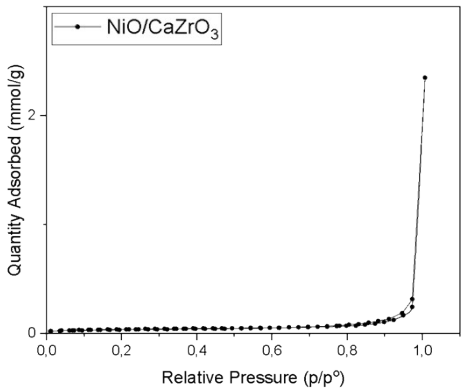

d)

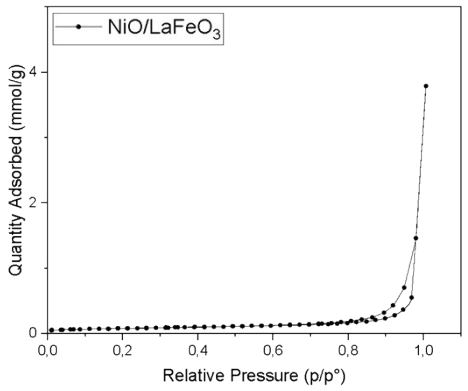

2. MEASUREMENTS OF THE REDUCED SAMPLES

FIG. A.3- XRD pattern of post-reduction experiment on NiO/Al_2O_3 catalysts (a), $NiO/MgAl_2O_4$-Al_2O_3 (b), $NiO/CaZrO_3$ (c), $NiO/LaFeO_3$ (d) (H_2-TPR heating from room temperature to 900 °C) and of $NiO/LaFeO_3$ (d) (H_2-TPR heating from room temperature to 600 °C) (in black), and their respective pre-reduction catalysts (in red).

b)

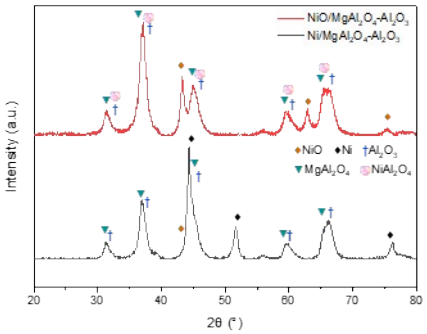

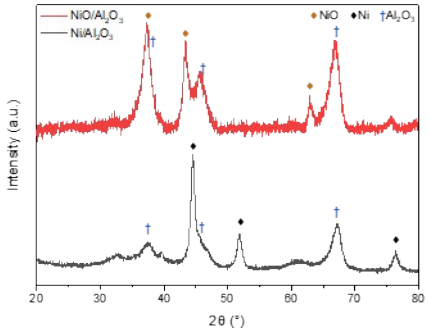

a)

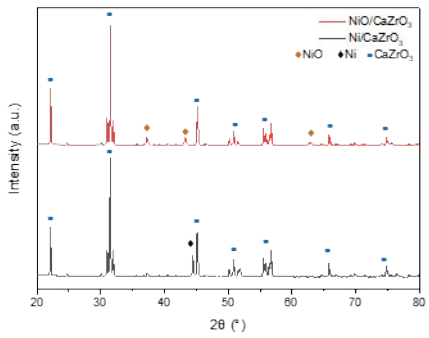

c)

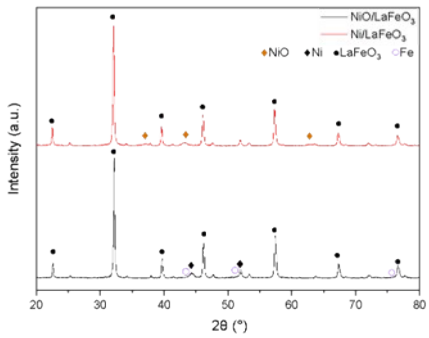

d)

e)

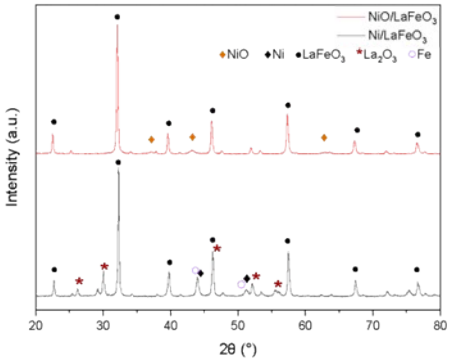

Sample	Metal Dispersion (%)
Ni/Al_2O_3	0.31%
$Ni/MgAl_2O_4$-Al_2O_3	0.36%
$Ni/CaZrO_3$	1.66%
$Ni/LaFeO_3$	0.26%

TABLE A.1- Nickel Dispersion for all samples

TABLE A.2 -H_2 quantity (cm^3/g) employed in TPR measurements and evaluation of the experimental quantity of NiO reduced, as well as the theoretical quantity of NiO present in each sample and the calculated percentage of NiO reduced in each sample.

Sample	Quantity H_2 (cm^3/g)	m_{NiO}/ g	$m_{NiO\ teorico}$/g	$\%_{NiO\ ridotto}$

NiO/Al_2O_3	39.08	0.13	0.16	79.83
$NiO/MgAl_2O_4$-Al_2O_3	45.41	0.15	0.17	91.39
$NiO/CaZrO_3$	54.76	0.18	0.17	110.34
$NiO/LaFeO_3$	55.72	0.19	0.17	109.33

The table shows that perovskites samples allowed the complete reduction of NiO, with an error due to the semiquantitative nature of the evaluation. For alumina-based samples, NiO reduced was evaluated as 20-30% less than perovskite-based samples. This might be due to the presence of the spinel $NiAl_2O_4$, which needs high temperatures to be reduced.

FIG. A.4- SEM-EDX maps of Ni/Al_2O_3 (a), $Ni/MgAl_2O_4$-Al_2O_3 (b), $Ni/CaZrO_3$ (c) and $Ni/LaFeO_3$ (d) catalysts after H_2-TPR.

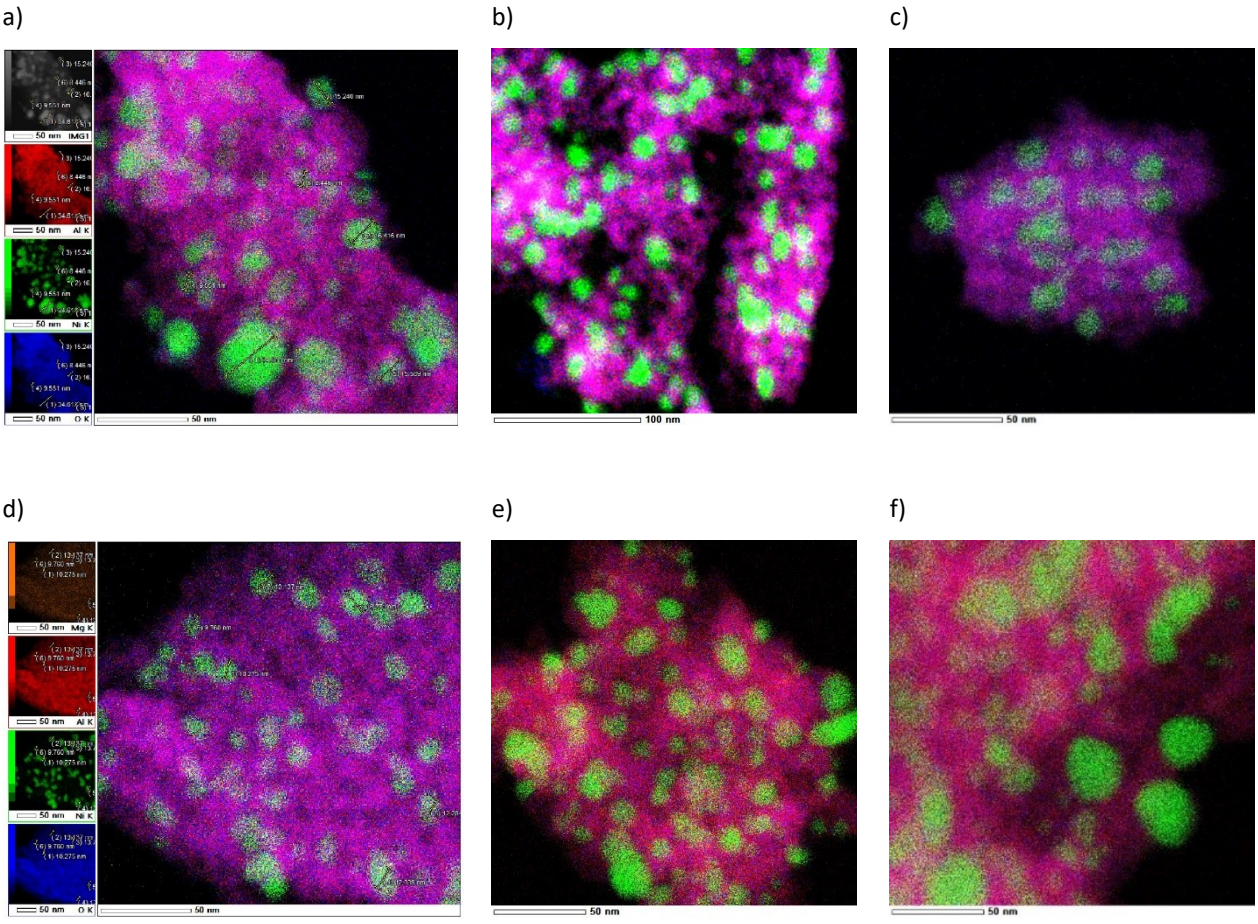

g)

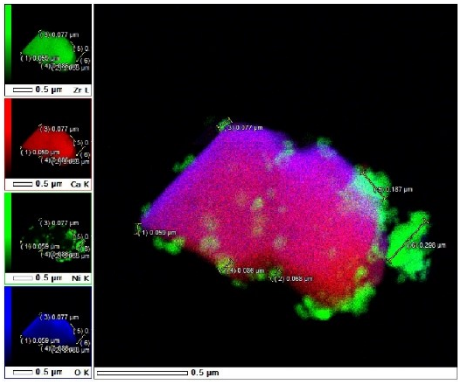

h)

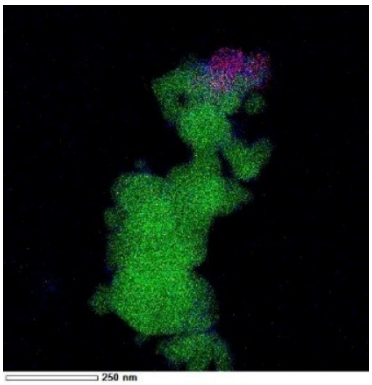

i)

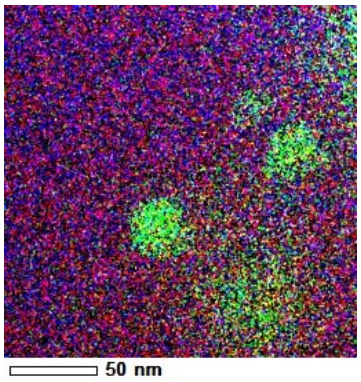

j)

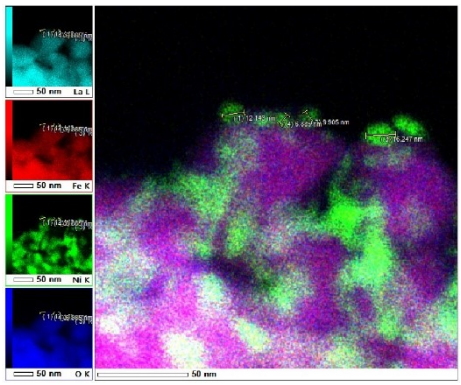

k)

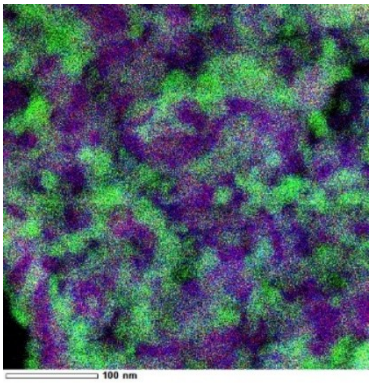

l)

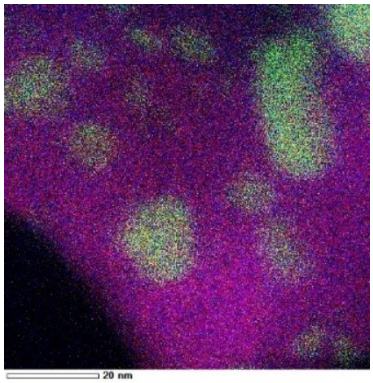

FIG. A.5- Ni 2p photopeaks with the fitting obtained from the different contributions of Ni species following spin-orbital splitting rules for Ni/Al_2O_3 (a) and $Ni/MgAl_2O_4$-Al_2O_3 (b) samples (after H_2-TPR).

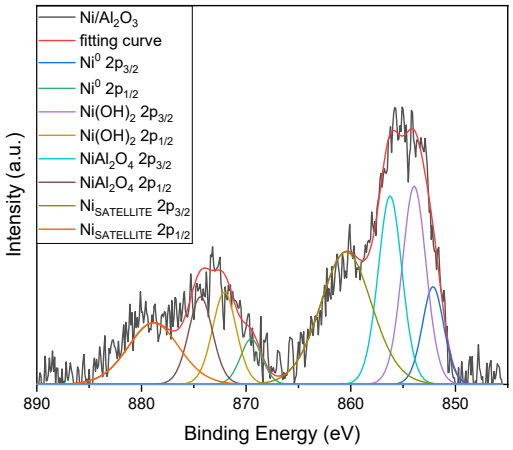

a)

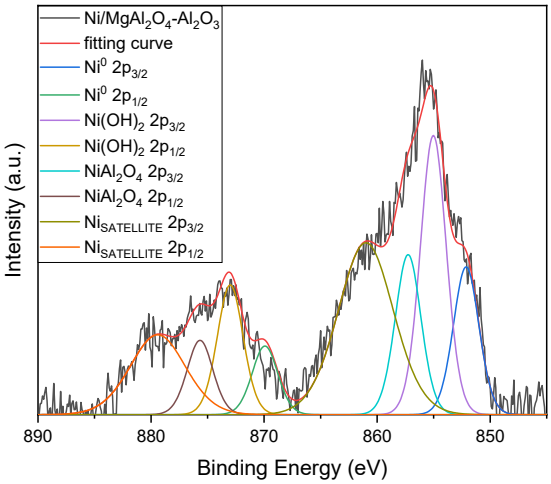

b)

3. XPS STUDY

TABLE A.3- Binding energy position (BE) and Area of XPS peak fitting contributions.

	Fe^0 Fe2p3/2	Fe^0 Fe2p1/2	$LaFeO_3$ Fe2p3/2	$LaFeO_3$ Fe2p1/2
$Ni/LaFeO_3$				
BE (eV)	706.72	718.20	710.26	723.20
A (CPS.eV)	2664.03	1089.47	17591.36	7718.61

	Ni^0 Ni2p3/2	Ni^0 Ni2p1/2	$Ni(OH)_2$ Ni2p3/2	$Ni(OH)_2$ Ni2p1/2	$NiAl_2O_4$ Ni2p3/2	$NiAl_2O_4$ Ni2p1/2	Ni sat. Ni2p3/2	Ni sat. Ni2p1/2
Ni/Al_2O_3								
BE (eV)	851.84	869.22	853.64	871.77	855.94	874.05	860.14	878.55
A (CPS.eV)	3391.14	1575.97	7628.25	3545.08	7254.35	3371.31	10930.02	5079.42
$Ni/MgAl_2O_4$-Al_2O_3								
BE (eV)	852.13	869.93	855.03	873.00	857.26	875.67	861.00	879.41
A (CPS.eV)	7846.74	3646.662	14936.24	69.4132	8559.51	3977.86	19694.20	9152.00

	Al_2O_3 Al2p3/2	Al_2O_3 Al2p1/2	$NiAl_2O_4$ Al2p3/2	$NiAl_2O_4$ Al2p1/2	$MgAl_2O_4$ Al2p3/2	$MgAl_2O_4$ Al2p1/2	Mg^0 Mg1s	$MgAl_2O_4$ Mg1s
Ni/Al_2O_3								
BE (eV)	73.57	74.18	74.67	75.44				
A (CPS.eV)	11808.111	5919.89	2358.50	1182.41				
$Ni/MgAl_2O_4$-Al_2O_3								
BE (eV)	73.18	73.68	74.13	74.64	75.20	75.74	1302.93	1305.32
A (CPS.eV)			96.1121	4818.49	2046.38	1025.93	20144.23	8580.86

	C=C bond C1s	C-C bond C1s	C-O-C bond C1s	O=C-O bond C1s
Ni/Al_2O_3				
BE (eV)	284.45	284.73	285.23	289.37
A (CPS.eV)	62122.64	25467.96	52836.89	13424.96
$Ni/MgAl_2O_4$-Al_2O_3				
BE (eV)	284.46	284.75	285.06	288.89
A (CPS.eV)	64453.52	5215777.87	55251.15	13375.45
$Ni/CaZrO_3$				
BE (eV)		284.71	287.16	290.13
A (CPS.eV)		12466.65	3398.47	547.53
$Ni/LaFeO_3$				
BE (eV)	284.51	284.81	286.31	288.48
A (CPS.eV)	57215.80	17367.25	20425.33	6113.34

4. CATALYTIC TESTS

TABLE A.4- TOF_{CH4} and TOF_{CO2} of of Ni/Al_2O_3, $Ni/MgAl_2O_3$-Al_2O_3 $Ni/CaZrO_3$, $Ni/LaFeO_3$ for 5 % CH_4, 5 % CO_2, 1 % NO in Ar ([a]) and 25 % CH_4, 25 % CO_2, 1 % NO in Ar ([b]) gas mixtures, calculated at t=200 min (time at which conversions were stable over time).

	Dispersion (%)	SSA (m^2/g)	TOF_{CH4}[a] (s^{-1})	TOF_{CH4}[b] (s^{-1})
Ni/Al_2O_3	0.31	105	12	102
$Ni/MgAl_2O_4$-Al_2O_3	0.36	62	6.5	81
$Ni/CaZrO_3$	1.66	3	0	0
$Ni/LaFeO_3$	0.26	6	23	62

	TOF_{CO2}[a] (s^{-1})	TOF_{CO2}[b] (s^{-1})	NO conversion rate[a*] (%)	NO conversion rate[b*] (%)
Ni/Al_2O_3	14	102	100	100
$Ni/MgAl_2O_4$-Al_2O_3	8.4	90	100	100
$Ni/CaZrO_3$	1.4	0	100	100
$Ni/LaFeO_3$	23	115	100	100

*complete NO conversion to N_2

FIG. A.6- Extended XPS spectra of post-reaction NiO/Al_2O_3, $NiO/MgAl_2O_4$-Al_2O_3, $NiO/CaZrO_3$ and $NiO/LaFeO_3$ catalysts.

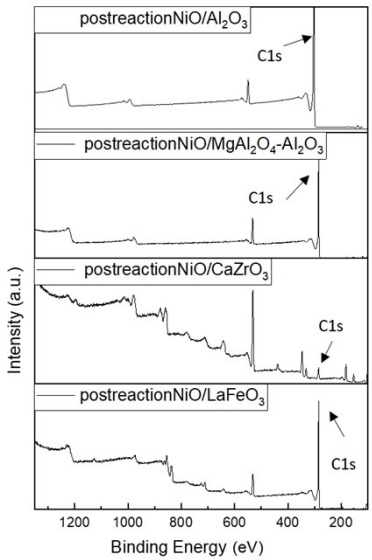

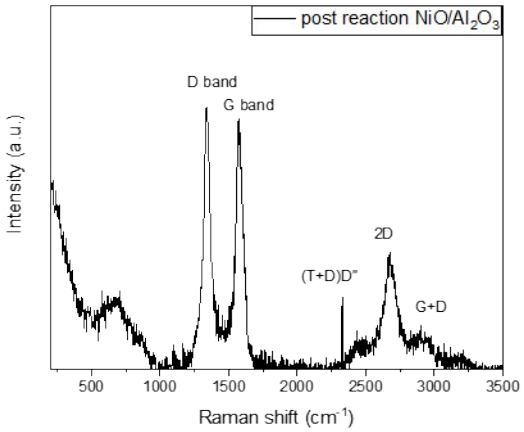

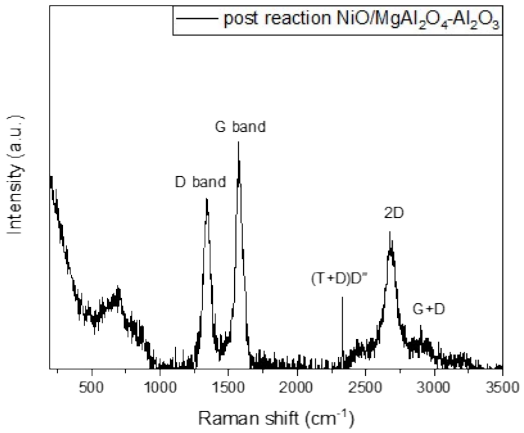

FIG. A.7.- Raman spectra for NiO/Al_2O_3, $NiO/MgAl_2O_4$-Al_2O_3 and $NiO/LaFeO_3$ catalysts. Spectra were acquired with focus 50X in a range between 200 and 3500 cm^{-1} except in $NiO/LaFeO_3$ spectra, where the acquisition range was reduced to 1000-2500 cm^{-1} to obtain a comparable resolution with the other spectra and minimize $LaFeO_3$ fluorescence issues.

a)

b)

c)